Development of Spatial Channel Model and Extended Spatial Channel Model for MIMO Applications

Raveesh Hegde [1], Dr. Geetha K.S.[2]
Department of Electronics and Communication
RV College of Engineering, Bangalore-560059

Abstract :

A MIMO Spatial Channel Model (SCM) applicable for 2 GHz carrier frequency and 5 MHz bandwidth channels is presented. The model provides a statistical description of spatial and temporal parameters pertaining to 3 different MIMO radio propagation environments namely suburban macro, urban macro and urban micro. A methodology is provided to model the fast fading channel coefficients between a base station and a mobile receiver based on sum of sinusoids method. Later, extension to the baseline model is provided to make it suitable for 5 GHz carrier frequency and 100 MHz bandwidth channels. The accuracy of the model is further enhanced by incorporating time varying model parameters.

I. Introduction to MIMO channel models

Multiple Input Multiple Output (MIMO) wireless communication techniques have attracted a great deal of attention in recent years due to their increased spectral efficiency, throughput and quality of service. In MIMO systems, multiple antennas are used at both transmitting and receiving end. The use of multiple antennas at the transmitter and the receiver in a wireless communication link opens a new dimension-space. Each pair of transmit and receive antenna provides a signal path from transmitter to the receiver which is called spatial channel. By sending signals that carry the same information through different spatial channels multiple independently faded replicas of the data symbol can be obtained at the receiver end, hence more reliable reception is achieved. Thus by optimally exploiting the spatial diversity of multiple propagation paths existing in a rich scattering environment, MIMO systems have become the most promising technology in meeting the increasing demand for better spectral efficiency and higher user bit rates. It is the radio propagation channel that determines crucially the characteristics of the entire MIMO system. Therefore accurate modeling of MIMO channels is an important prerequisite for MIMO system design, simulation, and deployment. With respect to MIMO system development, MIMO channel models serve a twofold purpose. First, a MIMO channel model can be used in the design of a MIMO system. This includes the design of an optimal signaling scheme, detection scheme, and space–time code etc. The same model can often be used to test a given system. In this case, the model acts as a channel simulator. We can generate exemplary channels using the model and use them to test the performance of a given system.

Earlier theoretical research on MIMO channel models utilized simple narrowband fading channel models such as Rayleigh and Rician. They were based on the assumption that individual paths in the MIMO channel are independent. Over the course of many experimental studies, it was found that, in many practical cases, this assumption was not accurate, since there is a significant space, time and frequency correlations among the multipaths of the channel. Thus, these analytical channel models were oversimplified and clearly inappropriate for system-level performance simulations [1].

To accurately emulate real world conditions, channel models must reproduce proper space, time and frequency correlations [2]. There have been different approaches to model this correlated behavior of the channel. In [3], Claude and Bruno describe various approaches for designing MIMO channel models. **Physical channel models** characterize an environment on the basis of electromagnetic wave propagation by describing the multipath propagation between the location of the transmit (Tx) array and the location of the receive (Rx) array. They explicitly model wave propagation parameters like the complex amplitude, AoD, AoA

and delay of a MPC. More sophisticated models also incorporate polarization and time variation. Depending on the chosen complexity, physical models allow for an accurate reproduction of radio propagation. WINNER MIMO channel model standardized by 3GPP AdHoc group is an example of physical MIMO channel model. **Analytical channel models** characterize the impulse response (equivalently, the transfer function) of the channel between the individual transmit and receive antennas in a mathematical/analytical way without explicitly accounting for wave propagation. A typical analytical model will mathematically express the MIMO channel matrix as a function of a random Gaussian-fading matrix and various channel correlations or steering vectors. Analytical models are very popular for synthesizing MIMO matrices in the context of system and algorithm development and verification. But they only provide a framework, but do not give fully quantitative information. Kronecker model, Weichselberger model are the examples of analytical channel models.

In [4] Larry et. al. deduce a statistical model for the distribution of rms delay spread within a cellular environment, including the effects of base-to-mobile distance, environment type (urban, suburban, rural, and mountainous areas), and the correlation between delay spread and shadow fading. It presents an empirical evidence, drawn from a wide array of published reports, which gives strong support to the log normal behavior of the rms delay spread.

In [5], H M Foster et al. suggest that it would be useful to divide the propagation effect into different categories. The categories were selected to be line of sight (LOS) and non-LOS streets. This made the characterization of the propagation phenomena simpler. Propagation along LOS and non-LOS roads was found to be dependent on width of the road, density of buildings on either side of the road and the distance away from the transmitter site. The current implementation uses the same approach to model the urban microcell environment.

In [6], George Calcev develops a MIMO spatial channel model and compares the simulated CDF graphs of RMS Delay Spread and RMS Angle Spread with the measured CDFs in the 3 SCM scenarios. Also it investigates the capacity of MIMO systems at different transmitter receiver configurations and different SNRs in three different scenarios. It was found that while maintaining reasonable computational complexity, the simulated results were able to match the reported measurement data in the literature.

In [7], P Lusina Et. al. develop a MIMO spatial channel model and compare it with the METRA Analytical Spatial Channel Model (A-SCM), and the correlation-based Long Term Evolution (LTE) channel model. The models are evaluated based on antenna element separation, array orientation, and angle spread. The impact of mutual coupling is also considered. The statistical assumptions used to generate the SCM model are in agreement with measurements from the literature. However, compared to the other channel models, SCM has a higher implementation complexity. Furthermore, its ray-based nature makes it difficult to isolate the influence of individual parameters on the performance.

Recently, demand has been rising for enhanced channel models that include not only the static channel behavior but also dynamic and time-variant channel behavior. In [8], K Saito proposes a Dynamic MIMO Channel Model. In this model, the dynamic properties of rays such as the ray's birth time, death time, and propagation parameter drift are estimated using Rao-Blackwellized particle filter. It was proved experimentally that the proposed dynamic channel model yields Angle of Arrival and Angle of Departure attributes, spread and auto-correlation, that agree with data measured in an urban environment well. But this paper fails to provide an exact model of the polarization effects produced by the channel.

One of the first attempts to include polarization effects into the MIMO channel models were made by Shafi et al. in [9] who extended the simple 2-D antenna pattern of the MIMO channel model to a dual-polarized 3-D pattern. This method was then also adopted for the WINNER model. However, Shafiet al.'s approach did not include a geometry-based method to calculate the cross-polarization effects. Instead, the cross polarization ratio (XPR) was incorporated statistically where the parameters were derived from measurements. This statistical approach is shown to lead to correct results for the cross-polarization discrimination (XPD) in case of a well-balanced statistical mixture between LOS and NLOS scenarios in an indoor environment. However, the distribution of singular values which is better suited for characterizing the multi-stream capabilities of MIMO channels has not been considered.

In [10], Stephan et. al. propose a new method to increase the accuracy of MIMO channel models by predicting the polarization state of a microwave link based on findings in the field of optics. This method was verified by cross-polarized MIMO measurements at 2.6 GHz with sixteen transmitters and ten receivers in an urban macro-cell environment under strong LOS conditions in downtown Berlin, Germany. Comparisons of simulation and measurement results showed that the coefficients of the polarized LOS channel can be predicted very well by the new method. Measured capacities at 10-dB signal-to-noise ratio (SNR) were in between 14.2 and 19.1 b/s/Hz values that can be predicted by the channel model with more than 90% accuracy.

In [11], Ernst Bonek discusses about the challenges that still persist in MIMO channel modeling. The author points out that modeling a highly non stationary channel is a challenging task. Along with that, vehicle to vehicle MIMO channel modeling, diffuse multipath modeling caused by multiple reflections and interference modeling are the emerging problems in MIMO channel modeling. The author opines that geometry based stochastic models are well suited in meeting these requirements.

II. Development of Spatial Channel Model

Spatial channel model distinguishes between three radio propagation environments.

1. Suburban Macro Environment

The suburban macrocell scenario describes a rural/suburban area with generally residential buildings and structures. The vegetation and any hills in the area are also assumed not to be too high. The BS antenna position is high, well above local clutter. As a result, the AS and DS are relatively small. In addition, the base-to-base distance is approximately 3 km.

2. Urban Macro Environment

The urban macro cellular environment describes large cells in areas with urban buildings of moderate heights in the vicinity and significant scattering. The BS antennas are placed at high elevations, well above the rooftops of any buildings in the immediate vicinity. The distance between BSs is again about 3 km. This scenario assumes moderate to high ASs at the BS and also large DSs. In urban environments, street canyon effects, i.e., wave propagation down relatively narrow streets with high buildings on both sides may be important in some cases and depending on their probability of occurrence, may lead to deviations from the generic urban macro cell case. Thus, street canyon effects are treated as optional extensions to the urban macro scenario. Another important effect, also treated as an option in this scenario, is the existence of additional clusters of energy due to far scatterers originating from high buildings.

3 Urban Micro Environment

In contrast to the above scenario, the urban microcell scenario describes small urban cells with inter base distances of approximately 1 km. Base antennas are located at rooftop level and therefore large ASs are expected at the BS, even though the DS is only moderate. In the case of macrocell scenarios discussed above, due to the relatively large area allocated to each BS, the fraction of locations in the cell with the chance to have a line-of-sight (LOS) component from the BS is small. Thus, for simplicity such channels are not modeled in the macrocell cases. However, for smaller cells, as in the case of microcell scenario, the users with LOS components cannot always be neglected.

The current implementation uses ray based approach in developing the spatial channel model. In this approach the propagation of radio waves is modeled in terms of discrete reflections and scatterings. The following figure 1 (source: Reference [11]) shows the various angle parameters considered in the implementation. The figure shows one Base Station (BS) and one Mobile Station (MS) and only one cluster of scatterers for simplicity.

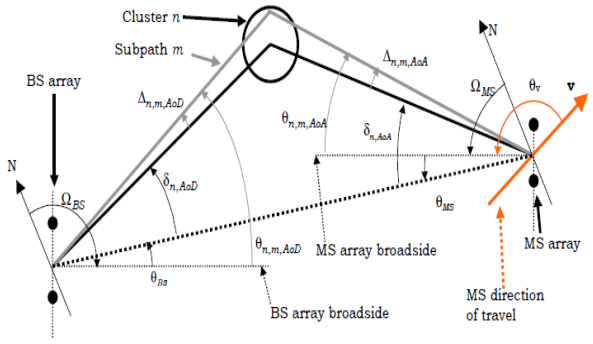

(Figure 1. Angle parameters of SCM)

Ω_{BS} BS antenna array orientation, defined as the difference between the broadside of the BS array and the absolute North (N) reference direction.

θ_{BS}	LOS AoD direction between the BS and MS, with respect to the broadside of the BS array.
$\delta_{n,AoD}$	AoD for the *n*th ($n = 1 \ldots N$) path with respect to the LOS AoD θ_0.
$\Delta_{n,m,AoD}$	Offset for the *m*th ($m = 1 \ldots M$) subpath of the *n*th path with respect to $\delta_{n,AoD}$.
$\theta_{n,m,AoD}$	Absolute AoD for the *m*th ($m = 1 \ldots M$) subpath of the *n*th path at the BS with respect to the BS broadside.
Ω_{MS}	MS antenna array orientation, defined as the difference between the broadside of the MS array and the absolute North reference direction.
θ_{MS}	Angle between the BS-MS LOS and the MS broadside.
$\delta_{n,AoA}$	AoA for the *n*th ($n = 1 \ldots N$) path with respect to the LOS AoA $\theta_{0,MS}$.
$\Delta_{n,m,AoA}$	Offset for the *m*th ($m = 1 \ldots M$) subpath of the *n*th path with respect to $\delta_{n,AoA}$.
$\theta_{n,m,AoA}$	Absolute AoA for the *m*th ($m = 1 \ldots M$) subpath of the *n*th path at the MS with respect to the BS broadside.
v	MS velocity vector.
θ_v	Angle of the velocity vector with respect to the MS broadside

Once the scenario has been chosen and the locations of the N_{BS} base-stations with the desired geometry and inter-base distances have been determined, one may start instantiating users in the area of interest. This entails first randomly generating the user locations. In addition, one needs to specify other user-specific quantities, such as their velocity vector v, with its direction θ_v drawn from a uniform [0, 360◦) distribution. Also, the specifics of the MS antenna or antenna array have to be determined, such as array orientation, MS, also drawn from a uniform [0, 360◦) distribution, polarization, etc. It should be stressed that while the velocity of a particular MS is generally assumed to be non-zero, it is assumed here that the macroscopic and mesoscopic parameters do not vary over the duration of a simulation run. However, the velocity and position of the MS directly affects the microscopic parameters (e.g., the channel coefficients). This assumption does not allow the model to accurately treat the behavior of some users over the duration of a simulation, since it does not describe dynamical hand-off situations or the passage of a particular user through different shadowing regions. However, it is expected that the statistics at a system level will not be affected.

To model the path loss, SCM employs the following path loss models. For a given user, the pathloss is a fixed multiplicative factor which is applied to all N multipath components.

1. The macrocell pathloss is based on the modified COST231 Hata urban propagation model:

$$PL[dB] = (44.9 - 6.55\log_{10} h_{bs})(\log_{10}(d) - \log_{10}(1000)) + 46.3 + 33.9\log_{10}(f_c) - 13.82\log_{10}(h_{bs}) - 3.2(1.07 + \log_{10} h_{ms})^2 + 4.97 + C \quad (1)$$

where the BS antenna height is h_{BS} = 32m, the MS antenna height is h_{MS} = 1.5m, the carrier frequency is f_c =1900MHz, *d* is the distance between the BS and MS in meters, and *C* is a constant factor (*C* = 0dB for suburban macro and *C* = 3dB for urban macro). The resulting pathlosses for suburban and urban macro environments are respectively,

$$PL = 31.5 + \log_{10}(d) \quad \text{and} \quad PL = 34.5 + \log_{10}(d). \quad (2)$$

The distance *d* is at least 35m.

2. The microcell NLOS pathloss is based on the COST 231 Walfish-Ikegami NLOS model with the following parameters: BS antenna height 12.5m, building to building distance 50m, street width 25m, MS antenna height 1.5m, orientation 30deg for all paths. With these parameters, the equation simplifies to:

$$PL(dB) = -55.1 + 38*\log10(d/m) + (24.5 + 1.5*f/925MHz)*\log10(f/MHz) \quad (3)$$

The resulting pathloss at 1900 MHz is: $PL(dB) = 34.5 + 38*\log10(d/m)$, where *d* is in meters. The distance d is at least 20m. A bulk log normal shadowing applying to all sub-paths has a standard deviation of 10dB.

3.The microcell LOS pathloss is based on the COST 231 Walfish-Ikegami street canyon model with the same parameters as in the NLOS case. The pathloss is

$$PL(dB) = -35.4 + 26*\log10(d/m) + 20*\log10(f/MHz) \quad (4)$$

The resulting pathloss at 1900 MHz is *PL*(*dB*) = 30.2 + 26*log10(d/m), where *d* is in meters. The distance *d* is at least 20m. A bulk log normal shadowing applying to all sub-paths has a standard deviation of 4dB.

The following section discusses how different parameters used in the development of spatial channel model are modeled.

i. Path Delays

The random delays of the paths have been seen experimentally to follow an approximate exponential distribution. Thus they can be expressed as

$$\tau_n' = -r_{DS}\sigma_{DS}\ln z_n \qquad n = 1,\ldots,N \qquad (5)$$

where z_n (n = 1, ...,N) are i.i.d. random variables with uniform distribution U(0, 1) and σ_{DS} is the standard deviation of the delay spread and r_{DS} is a constant whose value is 1.4 for suburban macrocell and 1.7 for urban macrocell.

In case of the urban microcellular environment, the fact that the BS antennas are now positioned at roof-top level results in blurring the distinction between clusters and paths. This requires a different approach in dealing with delay. In this case delays are IID random variables drawn from a uniform distribution of 0 to 1.2 microseconds.

ii. Path Powers

Path powers follow exponential distribution. As the delay increases, power of the path decreases exponentially. Thus, the average powers of the N paths, in case of macrocell can be expressed as

$$P_n' = e^{\frac{(1-r_{DS})\cdot(\tau_{(n)}'-\tau_{(1)}')}{r_{DS}\cdot\sigma_{DS}}}\cdot 10^{-\xi_n/10},\ n = 1,\ldots,6 \qquad (6)$$

ξ_n for n = 1, ...,N are i.i.d. Gaussian random variables with standard deviation σ_{RND} = 3dB, signifying the fluctuations of the powers away from the average exponential behavior. This parameter is also necessary to produce a dynamic range comparable to measurements.

In case of microcell, powers can be expressed as

$$P_n = 10\text{^}(-\tau_n - 0.1z_n) \qquad (7)$$

Average powers are then normalized, so that the total average power for all N paths is equal to unity:

$$P_n = \frac{P_n'}{\sum_{j=1}^{6} P_j'}. \qquad (8)$$

iii.Angles of Departure (AoD):

The spatial character of the adopted channel has a relatively large (N = 6) number of paths, each with a small angle spread (set to 2 degree in the macrocell case and 5 degree in the microcell case). This model would be quite accurate in the limit of many paths, when the channel response approaches a continuum. For simplicity only N = 6 such paths are used. To satisfy the overall, narrowband angle spread of σ_{AS}, the distribution of angles of departure at the base station (BS) has to be specified. For simplicity, a Gaussian distribution with variance $\sigma_{AoD} = r_{AS}\sigma_{AS}$ is chosen. The value of the proportionality constant r_{AS} is equal to 1.2 for suburban macro case and 1.3 for urban macro case. Higher values of r_{AS} correspond to power being more concentrated in a small AoD or a small number of paths that are closely spaced in angle. Thus the values of the AoD are initially given by

$$\delta_n' \sim \eta(0, \sigma_{AoD}^2), \qquad n=1\ldots N \qquad (9)$$

In the microcell case, each of the N paths is assumed to arrive from independent directions. As a result, their AoD at the base station can be modeled as IID uniformly distributed random variables. For simplicity, the width of the distribution is kept finite, between−40 degree to +40 degrees. When the LOS model is used, the AoD for the direct component is set equal to the LOS path direction.

These variables are given in degrees and they are ordered in increasing absolute value.

iv.Angles of Arrival (AoA) :

Similar to the case of AoDs, a model is necessary for the statistics of the AoAs at the mobile station (MS). It was observed that the paths that come from or close to the LOS tend to have higher relative power. The measurements showed that the AoA at the MS has a truncated normal distribution with mean zero with respect to the LOS. The variance of each path depends on the path's relative power given by

$$\sigma_{n,AoA} = 104.12\left(1-\exp\left(-0.2175\left|10\log_{10}(P_n)\right|\right)\right) \qquad (10)$$

and P_n is the relative power of the *n*th path

v.Shadow fading, angle spread and delay spread

Shadow-fading fluctuations of the average received power are known to be log-normally distributed. Recently, for macrocell scenarios, the fluctuations in

delay and angle spread were shown to behave similarly. The reason is that these quantities are sums of powers of individual sub-paths times the square of their corresponding delay times or angles. Since the powers are log-normally distributed and sums of log-normal variables are (approximately) log-normal, this implies that angle-spreads and delay-spreads have log-normal distributions. This explanation of the observed lognormal behavior of the delay spread was first conjectured in [4]. This motivation of how angle spread and delay spread are lognormally distributed also suggests that they will be correlated with shadow fading and each other. Based on this log-normal behavior, the delay-spread $\sigma_{DS,n}$ angle-spread $\sigma_{AS,n}$ and shadow fading $\sigma_{SF,n}$ parameters of the signal from BS n, where n = 1, · · · ,N_{BS}, to a given user can be written as:

$$10\log10(\sigma_{DS},n) = \mu_{DS} + \sigma_{DS}X1_n$$

$$10\log10(\sigma_{AS},n) = \mu_{AS} + \sigma_{AS}X2_n$$

$$10\log10(\sigma_{SF},n) = \sigma_{SF}X3_n \qquad (11)$$

In the above equations $X1_n$, $X2_n$, $X3_n$ are zero-mean, unit variance Gaussian random variables. μ_{DS} and μ_{AS} represent the median of the delay-spread and angle-spreads in dB. Once $\sigma_{DS,n}$ and $\sigma_{AS,n}$ have been determined, they are used to generate the relative delays and mean angles of departure of the intra cluster paths.

VI. Modeling the fast fading channel coefficients

The fast-fading coefficients for each of the N paths are constructed by the superposition of M individual subpaths, where each subpath is modeled as a wave component. The m^{th} component (m = 1, . . . ,M) is characterized by a relative angular offset to the mean AoD of the path at the BS, a relative angular offset to the mean AoA at the MS, a power and an overall phase. M is fixed to 20 and all sub-paths have the same power P_n/M. The subpath delays are identical and equal to their corresponding path's delay. This simplification is necessary since the model has a limited delay resolution. The overall phase of each subpath is i.i.d. and drawn from a uniform [0, 2π) distribution. The channel transfer function between receiver u and transmitter s at path n and time t is determined by the superposition of a large number of sinusoidal sub-paths as follows:

$$h_{u,s,n}(t) = \sqrt{\frac{P_n\sigma_{SF}}{M}}\sum_{m=1}^{M}\begin{pmatrix}\sqrt{G_{BS}(\theta_{n,m,AoD})}\exp\left(j\left[kd_s\sin(\theta_{n,m,AoD})+\Phi_{n,m}\right]\right)\times\\ \sqrt{G_{MS}(\theta_{n,m,AoA})}\exp\left(jkd_u\sin(\theta_{n,m,AoA})\right)\times\\ \exp\left(jk\|\mathbf{v}\|\cos(\theta_{n,m,AoA}-\theta_v)t\right)\end{pmatrix} \qquad (12)$$

P_n is the power of the *n*th path

σ_{SF} is the lognormal shadow fading applied as a bulk parameter to the n paths for a given drop.

M is the number of subpaths per-path.

$\theta_{n,m,AoD}$ is the the AoD for the *m*th subpath of the *n*th path

$\theta_{n,m,AoA}$ is the the AoA for the *m*th subpath of the *n*th path

$G_{BS}(\theta_{n,m,AoD})$ is the BS antenna gain of each array element

$G_{MS}(\theta_{n,m,AoA})$ is the MS antenna gain of each array element

J is the square root of -1.

K is the wave number $2\pi/\lambda$ where λ is the carrier wavelength in meters.

d_s is the distance in meters from BS antenna element *s* from the reference (*s* = 1) antenna.

d_u is the distance in meters from MS antenna element *u* from the reference (*u* = 1) antenna.

$\Phi_{n,m}$ is the phase of the *m*th subpath of the *n*th path

$\|\mathbf{v}\|$ is the magnitude of the MS velocity vector

θ_v is the angle of the MS velocity vector

III. Spatial Channel Model Extended

Spatial channel model follows the so called 'drop based concept' in generating the MIMO channel matrix. A drop can be seen as a relatively short channel observation period over which parameters such as AOA, AOD, MS velocity, path powers, path delays etc are assumed to be constant. But as the MS moves, AOA of the paths, LOS direction, path delays and path powers vary. These short-term variations are not accounted for in SCM.

Well defined "Beyond 3G Systems" use carrier frequencies in the 5 GHz band and provide a bandwidth upto 100 MHz. The increased bandwidth has it's effect on fading, path delay, channel spatial

autocorrelation and capacity. This effect has to be considered in the further MIMO channel models.

The SCM path-loss model is based on COST-Hata-Model for Suburban and Urban Macro and COST-Walfish-Ikegami-Model for Urban Micro. But at 5 GHz, signals undergo additional path loss compared to 2 GHz. Also, the COST-Hata-Model was derived for the purpose of GSM coverage prediction and has a distance range of 1-20 km. The 5 GHz band on the other hand is likely going to be used for short-range high-throughput services. So, an alternative path loss model is necessary.

In SCM, line of sight (LOS) model is provided for urban micro scenario only. Since 5 GHz range is mainly used for close distance personal communications, there is a very high probability of LOS. So there is a need to extend the LOS and K factor model to macro scenarios as well.

To overcome all these limitations, following extensions are provided to the basic SCM developed in the previous section to obtain the Extended Spatial Channel Model (SCME).

1. Intra cluster delay spread

In SCM, all paths within a scenario have the same path azimuth-spread (AS). Equivalently, we set the path delay spread(DS) to be constant. In SCME, 20 sub-paths are split into subsets, denoted "mid-paths", which we then move to different delays relative to the original path. Even though a mid-path consists of multiple sub-paths, it remains a single tap (delay-resolvable component).This approach limits the diversity increase to reasonable values and avoids that single sub-paths become delay-resolvable. Furthermore, lumping together a number of sub-paths keeps the fading distribution of that tap close to Rayleigh and thus aids a potential implementation with a classic Gaussian-distributed number generator.

2. 5 GHz path loss models

The most significant difference between 2 GHz path loss models and 5 GHz path loss models can be attributed to different gains in free-space path-loss, which is 8 dB higher at 5 GHz compared to 2 GHz. Thus, a 5 GHz path-loss model that has an offset of 8 dB is proposed for SCME.

3. Time varying angle and path delays

In SCME, we assume that the positions of scatterers are fixed during a drop. As a consequence, the scatter angles as seen from the BS (angles-of-departure, AoDs) do not change, with the exception of the LOS AoD in LOS scenarios. This assumption is valid in many cases of practical interest. Based on the fixed-geometry assumption, the scatter angles as seen from the MS (angles-of-arrival, AoAs) as well as the sub-path delays change during a drop due to the MS movement. Similarly, the LOS directions from BS and MS ($\theta_{BS,k}$ and $\theta_{MS,k}$ respectively) vary in time.

4. Tapped delay line model

In the SCM, most parameters are defined by their PDFs. While this provides richness in variability, it can turn out to be a headache for accurate simulations as the simulation time grows exponentially with the number of random parameters. As a practical add-on, SCME defines a set of fixed values for the power, delays and angular parameters of the paths.

IV. Simulation Results

This section presents a number of plots which result from the implementation of SCM and SCME. The obtained results are compared with the 3GPP standard released by European Telecommunication Standards Institute (ETSI) [13] and it was concluded that the current implementation conforms to the above mentioned standard.

A.RMS Delay Spread

Figure 2 shows the CDF of RMS delay spread corresponding to the three environments defined in SCM. . RMS delay spread is larger for the lower antenna heights and increases with distance of the MS from the BS. DS increases by about 40% as the base station antenna is lowered below the rooftops. This can be explained by the fact that the higher antenna strengthens the strongest multipath in NLOS case and accordingly the direct path in LOS case relative to the reflected paths. Hence the power in the reflected paths is much smaller compared to the strongest path.

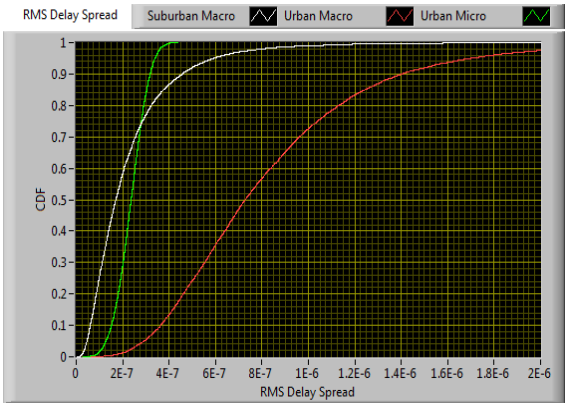

Figure 2 : RMS Delay Spread

B. RMS Angle Spread

A positive correlation is observed between the AS and DS. From a receiver point of view, the dependency between Angle Spread and Delay Spread means that the potential gains which can be achieved by using frequency and space diversity are highly correlated too.

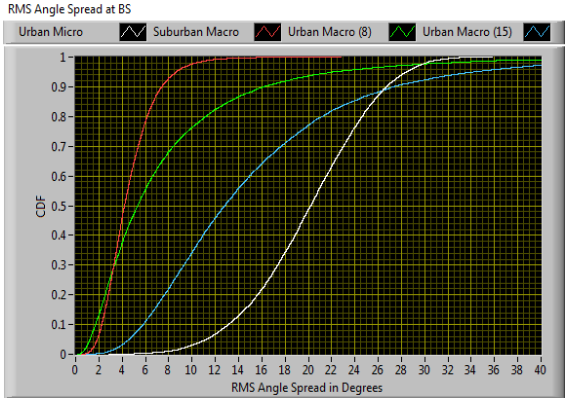

Figure 3 : RMS Angle Spread at the Base Station

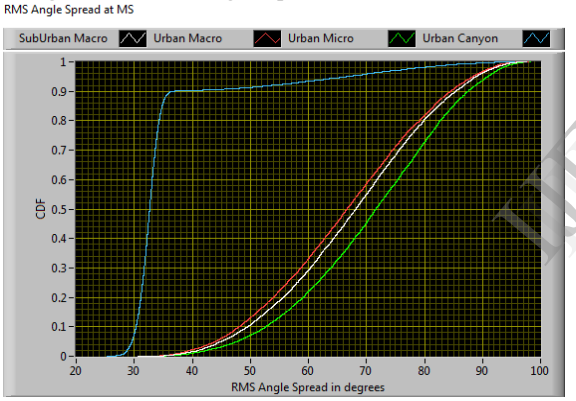

Figure 4 : RMS Angle Spread at the Mobile Station

C. Spatial Autocorrelation Function

Spatial autocorrelation function represents the correlation that exists among the received signal at different positions in the given environment. Reference [12] derives analytically that, ideally, spatial autocorrelation should follow Bessel function. In figure 5 and 6, deviation from the ideal behavior is observed due to the assumption of limited number of multipaths. As it is clear from figure 6, in the extended model, correlation was found to decay more quickly than in SCM.

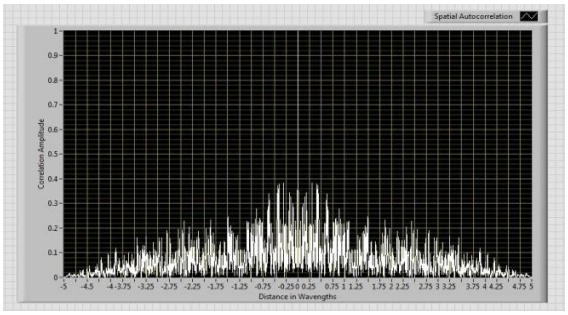

Figure 5. Spatial Autocorrelation- SCM

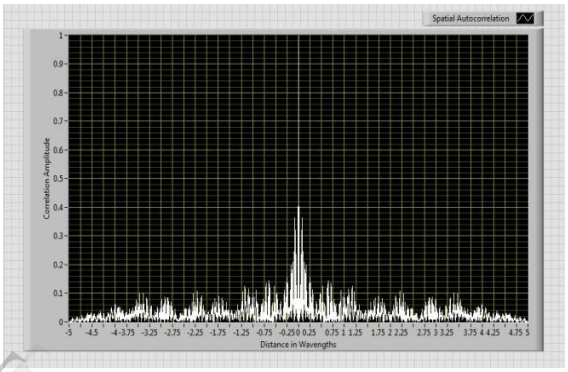

Figure 6. Spatial Autocorrelation function (SCME)

V. Conclusion

A comprehensive MIMO channel model, which takes into account both system and environmental parameters is developed. The model is suitable for 5MHz bandwidth systems at 2GHz carrier frequency range. Later, extension to the baseline model is provided to make it suitable for 5 GHz carrier frequency and 100 MHz bandwidth channels. The accuracy of the model is further enhanced by incorporating time varying model parameters. It was concluded that the extended model is able to reproduce the correlated behavior of the channel quite accurately.

References

1. Nelson Costa and Simon Haykin "Multiple Input Multiple Output Channel Models – Theory and Practice", *John Wiley Publications, 4th Edition, 2010*, ISBN 978-0-470-39983-5

2. Chengxiang Wang, Heriot Watt University "Modeling MIMO Fading Channels : Background, Comparison and Some Progress" *International Conference on Communications, Circuits and Systems Proceedings,Guilin*, 25-28 June 2006, pp 664-669

3.Claude Oestges and Bruno Clerckx "MIMO Wireless Communications-From Real World Propagation to Space

Time Code Design" *Academic Press, 1st Edition*, 2007, ISBN: 0-12-372535-6

4. Larry J. Greenstein,Fellow, IEEE,Vinko Erceg,Member, IEEE, Yu Shuan Yeh,Fellow, IEEE,and Martin V. Clark,Member, IEEE "A New Path-Gain/Delay-Spread Propagation Model for Digital Cellular Channels" *IEEE Transactions on Vehicular Technology, vol. 46, no. 2,* May 1997

5. H M Foster, S F Dehghan, R Steele, J J Stefanov and H K Strelouhov "Microcellular Measurements and Their Prediction" *1994 The Institution of Electrical Engineers. Printed and published by the IEE. Savoy Place,* London WCPR OBL, UK

6. George Calcev, Member, IEEE, Dmitry Chizhik, Bo Göransson, Member, IEEE, Steven Howard, Member, IEEE, Howard Huang, Senior Member, IEEE, Achilles Kogiantis, Member, IEEE, Andreas F. Molisch,Fellow, IEEE, Aris L. Moustakas,Senior Member, IEEE, Doug Reed,Member, IEEE, and Hao Xu,Member, IEEE "A Wideband Spatial Channel Model for System Wide Simulations" *IEEE Transactions on Vehicular Technology*, vol. 56, no. 2, March 2007.

7. P. Lusina, F. Kohandani, and S.M. Ali-Advanced Technology Research Research in Motion, Waterloo, Canada "Impact of MIMO Channel Models on Outage Capacity" *Radio and Wireless Symposium*, 2009. RWS '09. IEEE. 18-22 Jan. 2009 pp 171 – 174

8. K. Saito, K. Kitao, T. Imai, Y. Okano, and S. Miura," The Modeling Method of Time-Correlated MIMO channels using the Particle Filter", *2011 IEEE 73rd 2011 IEEE 73rd Budapest* 15-18 May 2011, pp 1 – 5

9. M. Shafi, M. Zhang, A. Moustakas, P. Smith, A. Molisch, F. Tufvesson, and S. Simon, "Polarized MIMO channels in 3-D: Models, measure-ments and mutual information,"*IEEE J. Sel. Areas Commun.*,vol.24, no. 3, pp. 514–527, March 2006

10. Stephan Jaeckel, Member, IEEE, Kai Börner, Student Member, IEEE, LarsThiele, Member, IEEE," A Geometric Polarization Rotation Model for the 3-D Spatial Channel Model", *IEEE Transactions on Antennas and Propagation*, vol. 60, no. 12, December 2012

11. Ernst Bonek, Institute of Telecommunications, Technische Universität Wien Wien, Austria "MIMO Propagation Channel Modeling" *7th European Conference on Antennas and Propagation (EUCAP 2013)*, Gothenburg, Sweden, 8-12 April 2013, ISBN :978-88-907018-1-8, pp 2488 - 2492

12. Hao Xu, Member, IEEE, Dmitry Chizhik, Howard Huang, Member, IEEE, and Reinaldo Valenzuela, Fellow, IEEE "A Generalized Space–Time Multiple-Input Multiple-Output (MIMO) Channel Model" *IEEE Transactions on Wireless Communications*, vol. 3, NO. 3, May 2004

13. ETSI TR 125 996 Universal Mobile Telecommunications System (UMTS): "Spatial channel model for Multiple Input Multiple Output (MIMO) simulations" *3GPP TR 25.996 Version 10.0.0 Release 10* (2011-04)